2.5 Analytics and Statistics

We jointly analyze the mean, the variation, and the extremes of the vertical distribution over each region. The purpose is to observe that the sources of aerosol plumes with similar mean heights may have very different variances, or may in general be similar, but have a set of extreme conditions which are quite different.

Furthermore, we employ a set of constant multiplicative wind spee factors as a means of testing the sensitivity of the model to the meteorology provided respectively by either MISR or NCEP. These values are applied in steps of 0.2 over the range from 0.8 to 1.6. This factor is applied both to the vertical wind as well as the horizontal wind, although it is not applied to both simultaneously. Although there is some connection between uncertainty in the wind and in the vertical temperature gradient, we do not consider this here, since there is no way simple way to couple this using reanalysis meteorology(Cohen et al. 2018).

3. RESULTS

3.1 Spatial-Temporal Distribution of the MISR Data

The spatial distribution of the climatological mean and the standard deviation of the MISR aerosol plume height in each 10km x 10km grid is given in Figure 1. Another way to look at this data is to analyze the vertical distribution over each region of interest. We have computed the amount of the total MISR points found within each 100m layer height, i.e. 0m to 100m, 100m to 200m, etc. as given in Table 2. These techniques allow us to understand and differentiate the different regions on the basis of their spatial and vertical climatology. We find that these results are different from previous attempts including those commonly accepted by the community as the gold standard.

As displayed in Figure 1a we can clearly analyze which areas have the largest impact on aerosol height, which specifically include southern and Central Africa, Central South America, Siberia, Northern Southeast Asia, Canada, and Northern Australia. However, there are some regions over which MISR has not captured what were otherwise expected to be areas with a significant aerosol vertical source, in specific those regions in the Sichuan Basin, Indonesia, and India. The reason may be due to meteorological factors, because pollutants emitted from local sources are mixed in with biomass burning plumes in the regions. Another possibility is that high levels of clouds that occur at the same time as the biomass burning in these regions may be masking their signal. Another consequence of these two rationales is that there are some regions where we find there are too many plumes, such as in Northern Australia, Eastern Europe, Eastern China, and the Northeastern USA, which may in fact be related to downwind transport from these areas, or mis-characterization of surface heat sources which are not from fires.

We determine that a significant amount of aerosol mass exists in the free troposphere over each region. Assuming the measured daily average boundary layer height can be represented by the range from 1000m to 2000m(Guo et al. 2016, Cohen et al. 2018), and has a central value of 1500m, we compute the fraction of the aerosol loading in the free troposphere of the regions, respectively (with all values representing a percent above the respective boundary layer height): (31,57,12); (64,35,1); (5.9,70,24.1); (22,51,27); (37,55.7,7.3);(50,45,5); (64.5,30,5.5); (37,36,27); (64,32,3.9); (29,46,25); (22,36,42); (63,32,5); (84,11,5); and (39,44,17), respectively. This set of results is important in three ways, first that in all regions, the amount in the free troposphere is more than in previous studies (which indicated the large majority of smoke remained within the boundary layer(Cohen et al. 2018)); secondly that there is a significant difference between different regions when the boundary layer is high, which will cause considerable divergence when the current generation of models are compared with measurements; and third, that the wide variation will. likely cause significant retrieval errors in aerosol products, including AOD.

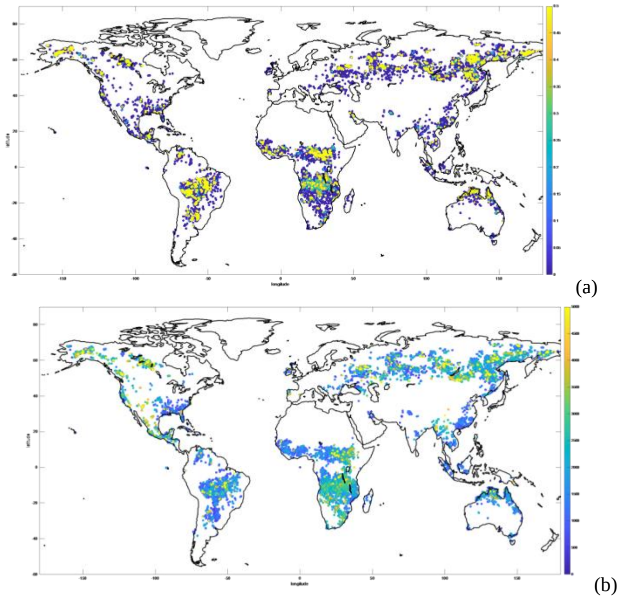

Figure 1. Climatological mean (a) and Climatological normalized standard deviation (b) of the daily average MISR plume height measurements, from January 2008 through July 2011.

With respect to the case of Central Canada, we find that both the boundary layer and the free troposphere both have a roughly similar amount of aerosol (58.3% in the boundary layer and 39% in the lower free troposphere). What is unique is that over this region, there is also a significant amount of aerosol (2.7%) found in the middle and upper free troposphere above 5km. The results in this region are consistent with primary forests being burnt at very high temperature.

	0-1k	1k-2k	2k-3k	3k-4k	4k-5k	>5k
Central Africa	30.9%	56.9%	9.9%	1.7%	0.3%	0.3%
Midwest Africa	64.4%	34.8%	0.6%	0.1%	0.0%	0.1%
Southern Africa	5.8%	69.8%	22.9%	1.2%	0.2%	0.1%
Central Siberia	21.8%	50.8%	22.0%	4.0%	0.8%	0.7%
Siberia and Northern China	36.8%	55.7%	5.9%	0.4%	0.2%	0.9%
Eastern Siberia	50.2%	44.7%	3.3%	0.7%	0.1%	0.9%
Western Siberia	64.7%	29.8%	3.9%	0.8%	0.3%	0.4%

Northern Southeast Asia	37.1%	35.6%	17.0%	7.3%	2.4%	0.6%
Northern Australia	64.3%	31.8%	2.6%	1.2%	0.1%	0.1%
Alaska	29.3%	45.8%	17.8%	5.6%	1.1%	0.5%
Central Canada	22.3%	36.0%	25.5%	9.7%	3.9%	2.7%
South America	63.1%	31.4%	4.4%	0.7%	0.1%	0.2%
Argentina	83.8%	11.1%	2.3%	2.3%	0.6%	0.0%
Eastern Europe	38.5%	44.1%	9.7%	4.5%	2.7%	0.5%

Table 2. Statistical summary of different height of MISR measurements during 2008-2011, over different regions

Furthermore, the vast majority of the other locations we cannot as readily draw a statistically significant conclusion about the nature of the heights. We find that in many cleaner regions (as determined by the profiles of NO2 from OMI) specifically in Siberia, Alaska, and Australia, the magnitude of the standard deviation of height is extremely large when compared with the plume height, making characterization complex. These regions sometimes have very severe fires, and at other times have low-temperature fires. However, we can observe from the NO2 profiles that the emissions do not vary greatly between the total emissions levels found under the different sets of aerosol height conditions. This tells us that a deeper understanding is required in order to understand the vertical aerosol distribution.

On the other hand, in those regions which have a higher loading of pollutants, such as in Central Africa, Southeast Asia, South America, etc. there is a more complex set of aerosol sources. These regions have a significant amount of biomass burning, but also have a rapidly increasing amount of urbanization and high population density. These urban sources will tend to mostly occur within the boundary layer. Therefore, we find that some of these regions have a higher standard deviation in aerosol height and hence are harder to characterize. However, a subset of these regions, in specific Southeast Asia and Western Central Africa, have a lower standard deviation and are found to have a very consistent aerosol height distribution during the latter parts of the local dry season. In all of these sets of cases however, we find that the simple model based on FRP and meteorology still does not perform well. This has a known theoretical basis however. Firstly, because these regions tend to have clouds at the same time as the burning. And secondly because in the case where there is a significant amount of absorbing aerosol near the top of boundary layer and extending into the lower free troposphere, its interaction with radiation is much stronger, and the lifetime of the aerosol will be enhanced. Furthermore, there may be interactions between the aerosols themselves with the dynamics, possibly providing a feedback further narrowing the aerosol plume height.

3.2 Sensitivity Tests of Wind Factor on Plume Rise Model

The statistical results of the plume rise model when applied to all of the regions from Table 3 in the respective order are found to have an aggregated mean height (and standard deviation) respectively of: 0.59km(0.22km), 0.60km(0.23km), 0.58km(0.23km), 0.87km(0.89km), 0.80km(0.64km), 0.68km(0.34km), 0.79km(0.95km), 0.73km(0.38km), 0.64km(0.29km), 1.39km(3.03km), 1.73km(2.19km), 0.50km(0.21km), 0.65km(0.25km), and 1.27km(2.67km).

Across all of these results, we find that the average modeled height is always lower than the average height of the measurements, with the range from 0.04km to 0.83 km. The regions with the best average height representation are found in Argentina (0.04km), East Europe (0.14km), West Siberia (0.16km), Alaska (0.18km), Central Canada (0.24km) and Northern Australia (0.26km).Those regions with a high average standard deviation are not considered further in this work.

A very interesting point is that most of the regions which have a reasonable average representation by the plume rise model are found at middle and high latitudes, and are regions which are generally cloud-free. This means that localized effects such as the fire-induced heating are more important, since they do not as frequently experience large-scale deep convection (like the tropics) and they also do not have as much bias in terms of FRP measurements being hindered (i.e. by cloud cover). Both these aspects lead to a more simplified dynamical plume mode being more suitable. The opposite is expected to be true in the regions which are found to have the largest difference between the mean height and plume rise model representation, such as in Africa, Southeast Asia, and the Amazon.

	Western Siberia	Alaska	Central Canada	Argentina	Eastern Europe
MISR data	0.95 *(0.77)*	1.57 *(0.91)*	1.97 *(1.26)*	0.69 *(0.70)*	1.41 *(1.05)*
Plume Model	0.79 *(0.95)*	1.39 *(3.03)*	1.73 *(2.19)*	0.65 *(0.25)*	1.27 *(2.67)*
VX=0.8	0.71 *(0.80)*	1.25 *(2.56)*	1.48 *(1.84)*	0.60 *(0.24)*	1.12 *(2.25)*
VX=1.2	0.86 *(1.09)*	1.52 *(3.48)*	1.96 *(2.51)*	0.69 *(0.27)*	1.41 *(3.07)*
VX=1.4	0.92 *(1.23)*	1.63 *(3.91)*	2.19 *(2.83)*	0.73 *(0.29)*	1.54 *(3.45)*
VX=1.6	0.98 *(1.36)*	1.74 *(4.33)*	2.41 *(3.13)*	0.76 *(0.30)*	1.67 *(3.82)*
UX=0.8	0.89 (1.20)	1.58 *(3.80)*	2.13 *(2.75)*	0.70 *(0.28)*	1.49 *(3.35)*
UX=1.2	0.71 *(0.79)*	1.26 *(2.52)*	1.46 *(1.81)*	0.61 *(0.24)*	1.12 *(2.22)*
UX=1.4	0.66 *(0.67)*	1.16 *(2.15)*	1.27 *(1.55)*	0.58 *(0.23)*	1.00 *(1.90)*
UX=1.6	0.62 *(0.59)*	1.08 *(1.88)*	1.13 *(1.35)*	0.55 *(0.22)*	0.92 *(1.66)*

Table 3. Statistics of (top row) measured MISR plume heights and (*standard deviations*) using daily data from 2008 to 2011; (second row) the plume rise model; and various sensitivity tests with the model as a function of vertical (VX) and horizontal (YX) velocity.

One important meteorological factor in terms of plume rise modeling is the wind speed, as shown in Table 3. Initially wind speed was assumed to be constant uniform over the entire vertical rise of the plume. However, given how high these plumes rise, such an assumption may no longer be valid, as winds in the lower free troposphere are frequently different from in the boundary layer. Therefore, a sensitivity analysis can help us to understand the impact of such assumptions on the model's ability to predict the plume heights. For Argentina, East Europe and West Siberia, the change of wind speed factor has little impact on the RMS (about 0.4, 0.8 and 0.7 respectively for Argentina, East Europe and West Siberia). But the best-fit wind factors (in terms of root mean square error (RMS)) are found to specifically be VX=1.6,RMS=1.10km for Central Canada and

VX=1.2,RMS=0.66km and UX=0.8,RMS=0.66km for West Siberia.

3.3 Modeled Aerosol Vertical Distribution

A comparison of the day-to-day modeled and measured heights for the best-fit regions is given in Figure 2. Firstly, most of the modeled values are found to fall within one standard deviation of the measured mean daily value over each region (the length of the error bars in the plot). Secondly, it is observed that the vast majority of the data is aggregated around certain times of the year as a function of each site, which in all cases belongs to the local dry season when FRP and stereo measurements are available. Thirdly, a significant amount of the total RMS error occurs when there are either extremely high measured values over 5km (indicating pyro-convection or other non-standard vertical atmospheric conditions) or when the modeled height is three times higher than the measured height and at the same time the measurement is located below 0.5 km (indicating that FRP is not the reason why the model is wrong).

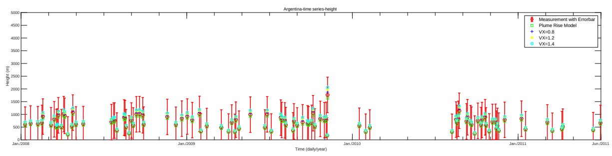
(a)
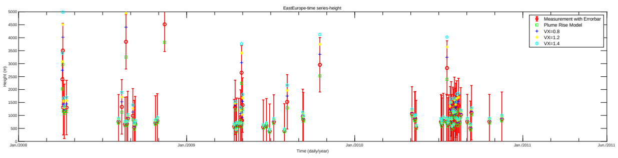
(b)
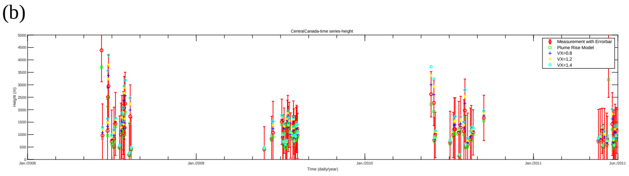
(c)
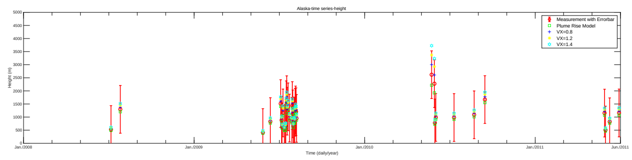
(d)
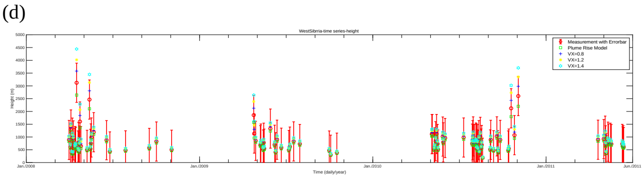
(e)
Figure 2. Comparison the time series of wind speed factors height, plume rise model height and measured height over five best-fit regions (a) Argentina; (b) East Europe; (c) Central Canada; (d) Alaska; (e) West Siberia.

4. DISCUSSION AND CONCLUSION

This work uses new data on the vertical distribution of aerosols and combines this with a simple plume rise model to estimate the vertical distribution of smoke plumes. We find that applying measurements of the daily mean and standard deviation of data over the whole world from MISR allows us to derive useful and meaningful characteristics of the vertical plume height over regions without significant cloudiness. We find that in non-tropical forests, such as Alaska, Argentine, and Siberia, the overall characteristics are stable, with a few dominating extreme events, including events lofting aerosols into the stratosphere. Over Africa and parts of Southeast Asia, we find that aerosols likely come from multiple sources include biomass burning, anthropogenic sources, and long-range transport, so that a significant amount of the total plume is found both below the boundary layer during part of the year, and above the boundary layer during other parts of the year.

While trying to understand the major cause of model uncertainty, we have discovered that uncertainties in the measured wind speed are significant. Over some regions, the model performs better when error in the wind measurements are random in nature, such as in Argentina and Central Canada. Over other regions, we find that a bias in wind speed allows for a best fit with measurements, including in Western Siberia, Alaska, and Eastern Europe. In terms of the most extreme events, our model when used with an enhanced wind factor of VX=1.4, is capable of reproducing the timing of the enhanced higher plume heights that are observed in Western Siberia (April 2008), Eastern Europe (September 2008), Alaska (May 2009), and Argentina (November 2009). Although this wind factor is not uniform everywhere and merely applying it uniformly will lead to other occurrences where the measured heights are severely overestimated. Over the rest of the world, the simple plume model approach is found to not be appropriate under any set of reasonable wind-speed conditions.

Conversely to other findings, we have not identified any statistically valid trend in the aerosol height distribution over the time series from 2008 to 2011. This indicates that a combination of the emissions and underlying processes controlling the vertical distribution have not changed much over the time of interest. Simultaneously, we also have determined contrary to the literature that the most extreme values measured (both for plumes above 5km and below 500m) are not well reproduced by the plume rise model, even though the FRP values have been measured in cloud-free conditions, indicating that there are other factors besides bias of the FRP and wind speed which are driving these more extreme conditions.

REFERENCES

Achtemeier, G. L., Goodrick S. A., Y. Liu, F. Garcia-Menendez, Hu, Y., Odman, M. T., 2011. Modeling Smoke Plume-Rise and Dispersion from Southern United States Prescribed Burns with Daysmoke. *Atmosphere*, 2(3), 358-388.

Cohen, J. B., 2014. Quantifying the occurrence and magnitude of the Southeast Asian fire climatology. *Environmental Research Letters*, 9(11), 114018.

Cohen, J. B., Lecoeur, E., Ng, D. H. L., 2017. Decadal-scale relationship between measurements of aerosols, land-use change, and fire over Southeast Asia. *Atmospheric Chemistry & Physics*, 17(19), 26895-26957.

Cohen, J. B., Ng, D. H. L., Lim, A. W. L., Xin, R. C. J., 2018. Vertical distribution of aerosols over the Maritime Continent during El Niño. *Atmospheric Chemistry & Physics*, 18(10), 7095-7108.

Cohen, J. B., Prinn, R. G., Wang C., 2011. The impact of detailed urban-scale processing on the composition, distribution, and radiative forcing of anthropogenic aerosols. *Geophysical Research Letters*, 38(10),264-265.

Diner, D. J., Beckert, J. C., Reilly, T. H., Bruegge, C. J., Conel, J. E., Kahn, R. A., Martonchik, J. V., Ackerman, T. P., Davies, R., Gerstl, S. A. W., Gordon, H. R., Muller, J. P., Myneni, R. B., Sellers, P. J., Pinty, B., Verstraete, M. M., 1998. Multi-angle Imaging SpectroRadiometer (MISR) instrument description and experiment overview. *IEEE Transactions on Geoscience and Remote Sensing*, 36(4), 1072-1087.

Freeborn, P. H., Wooster, M. J., Roy D. P., Cochrane M. A., 2014. Quantification of MODIS fire radiative power (FRP) measurement uncertainty for use in satellite- based active fire characterization and biomass burning estimation. *Geophysical Research Letters*, 41(6), 1988-1994.

Guo, J., Deng, M., Lee, S. S., Wang, F., Li, Z., Zhai, P., Liu, H., Lv, W., Yao W., Li X., 2016. Delaying precipitation and lightning by air pollution over the Pearl River Delta. Part I: Observational analyses. *Journal of Geophysical Research Atmospheres*, 121(11), 6472-6488.

Ichoku, C., Ellison L., 2014. Global top-down smoke-aerosol emissions estimation using satellite fire radiative power measurements. *Atmospheric Chemistry and Physics*, 14(13), 6643-6667.

Kahn, R. A., Li, W. H., Moroney, C., Diner, D. J., Martonchik, J. V., Fishbein, E., 2007. Aerosol source plume physical characteristics from space-based multiangle imaging. *Journal of Geophysical Research-Part D-Atmospheres*, 112, 1-20.

Kalnay, E., 1996. NCEP/NCAR 40-year reanalysis project. *Bulletin of the American Meteorological Society*, 77(3), 437-472.

Kauffman, J. B., Steele, M. D., Cummings, D. L., Jaramillo, V. J., 2003. Biomass dynamics associated with deforestation, fire, and, conversion to cattle pasture in a Mexican tropical dry forest. *Forest Ecology and Management*, 176(1-3), 1-12.

Kaufman, Y. J., Justice, C. O., Flynn, L. P., Kendall, J. D., Prins, E. M., Giglio, L., Ward, D. E., Menzel W. P., Setzer A. W., 1998. Potential global fire monitoring from EOS-MODIS. *Journal of Geophysical Research*, 103(D24), 32215-32238.

Mims, S. R., Kahn, R. A., Moroney, C. M., Gaitley, B. J., Nelson, D. L., Garay M. J., 2010. MISR Stereo Heights of Grassland Fire Smoke Plumes in Australia. *IEEE Transactions on Geoscience and Remote Sensing*, 48(1), 25-35.

Nelson, D. L., Garay, M. J., Kahn R. A., Dunst, B. A., 2013. Stereoscopic Height and Wind Retrievals for Aerosol Plumes with the MISR INteractive eXplorer (MINX). *Remote Sensing*, 5(9), 4593-4628.

Paugam, R., Wooster, M., Freitas S., Martin M. V., 2016. A review of approaches to estimate wildfire plume injection height within large-scale atmospheric chemical transport models. *Atmospheric Chemistry and Physics*, 16(2), 907-925.

Singh, N., Banerjee, T., Raju, M. P., Deboudt, K., Sorek-Hamer, M., Singh, R. S., Mall, R. K., 2018. Aerosol chemistry, transport, and climatic implications during extreme biomass burning emissions over the Indo-Gangetic Plain. *Atmospheric Chemistry and Physics*, 18(19), 14197-14215.

Tosca, M. G., Randerson, J. T., Zender, C. S., Nelson, D. L., Diner, D. J., Logan, J. A., 2011. Dynamics of fire plumes and smoke clouds associated with peat and deforestation fires in Indonesia. *Journal of Geophysical Research-Atmospheres*, 116(D8).

Trentmann, J., Luderer, G., Winterrath, T., Fromm, M. D., Servranckx, R., Textor, C., Herzog, M., Graf, H. F., Andreae, M. O., 2006. Modeling of biomass smoke injection into the lower stratosphere by a large forest fire (Part I), reference simulation. *Atmospheric Chemistry and Physics*, 6, 5247-5260.

Turquety, S., Logan, J. A., Jacob, D. J., Hudman, R. C., Leung, F. Y., Heald, C. L., Yantosca, R. M., Wu, S.,. Emmons, L. K, Edwards, D. P., Sachse, G. W., 2007. Inventory of boreal fire emissions for North America in 2004: Importance of peat burning and pyroconvective injection. *Journal of Geophysical Research-Atmospheres*, 112(D12).

Van Donkelaar, A., Martin, R. V., Levy, R. C., Da Silva, A. M., Krzyzanowski, M., Chubarova, N. E., Semutnikova, E., Cohen, A. J. 2011. Satellite-based estimates of ground-level fine particulate matter during extreme events, A case study of the Moscow fires in 2010. *Atmospheric Environment*, 45(34), 6225-6232.

Vernon, C. J., Bolt, R., Canty, T., Kahn, R. A. 2018. The impact of MISR-derived injection height initialization on wildfire and volcanic plume dispersion in the HYSPLIT model. *Atmospheric Measurement Techniques*, 11(11), 6289-6307.

Revised August 2019